

REAL TIME INSTRUMENTATION FOR PAVEMENT RUT MEASUREMENTS

by

Roger S. Walker, P.E.
Scott Wright
Wen-Ming Kuo

Research Report #1290-1F

conducted for

Texas Department of Transportation

in cooperation with the
U.S. Department of Transportation
Federal Highway Administration

June 1995

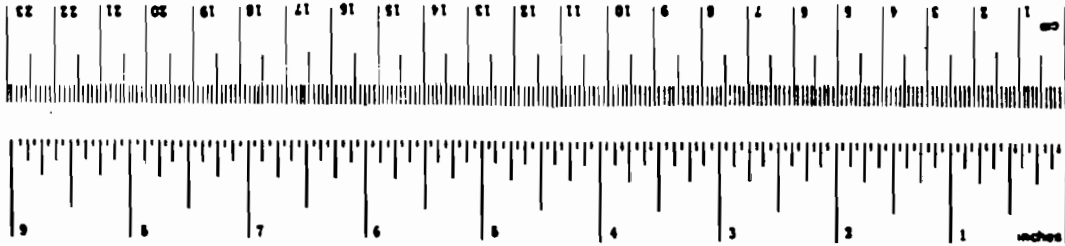
METRIC CONVERSION FACTORS

Approximate Conversions to Metric Measures

Symbol	When You Know	Multiply by	To Find	Symbol
LENGTH				
in	inches	2.5	centimeters	cm
ft	feet	30	centimeters	cm
yd	yards	0.9	meters	m
mi	miles	1.6	kilometers	km
AREA				
m ²	square inches	6.5	square centimeters	cm ²
ft ²	square feet	0.09	square meters	m ²
yd ²	square yards	0.8	square meters	m ²
mi ²	square miles	2.6	square kilometers	km ²
	acres	0.4	hectares	ha
MASS (weight)				
oz	ounces	28	grams	g
lb	pounds	0.45	kilograms	kg
	short tons (2000 lb)	0.9	tonnes	t
VOLUME				
cup	teaspoons	5	milliliters	ml
fl oz	tablespoons	15	milliliters	ml
c	fluid ounces	30	milliliters	ml
pt	cup	0.24	liters	l
qt	pints	0.47	liters	l
gal	quarts	0.98	liters	l
	gallons	3.8	liters	l
fl oz	cubic feet	0.03	cubic meters	m ³
yd ³	cubic yards	0.76	cubic meters	m ³
TEMPERATURE (exact)				
°F	Fahrenheit temperature	5/9 (after subtracting 32)	Celsius temperature	°C

Approximate Conversions from Metric Measures

Symbol	When You Know	Multiply by	To Find	Symbol
LENGTH				
mm	millimeters	0.04	inches	in
cm	centimeters	0.4	inches	in
m	meters	3.3	feet	ft
km	kilometers	1.1	yards	yd
		0.6	miles	mi
AREA				
cm ²	square centimeters	0.16	square inches	in ²
m ²	square meters	1.2	square yards	yd ²
km ²	square kilometers	0.4	square miles	mi ²
ha	hectares (10,000 m ²)	2.5	acres	ac
MASS (weight)				
g	grams	0.035	ounces	oz
kg	kilograms	2.2	pounds	lb
t	tonnes (1000 kg)	1.1	short tons	st
VOLUME				
ml	milliliters	0.03	fluid ounces	fl oz
l	liters	2.1	pints	pt
		1.06	quarts	qt
		0.26	gallons	gal
m ³	cubic meters	36	cubic feet	ft ³
		1.3	cubic yards	yd ³
TEMPERATURE (exact)				
°C	Celsius temperature	9/5 (then add 32)	Fahrenheit temperature	°F



* 1 in = 2.54 (exactly). For other exact conversions and more detailed tables, see NBS Mon., Publ. 758, Units of Length and Measure, Price \$2.25; SD Catalog No. C-1310 288.

IMPLEMENTATION

The Department currently uses Siometer's in most districts for pavement management and project data collection activities. The improved rutting capabilities developed in this research can and is currently being used to more quickly collect much more accurate information for PES and project specific applications. The rutting information is sent to a standard lap-top (IBM PC compatible) computer and can easily be accessed via floppy disks or downloaded to other PC compatible systems. The selection of more accurate equipment will be useful not only to Texas but other states.

In order to collect accurate rut data, which includes rutting generated by trucks, extensions outside the vehicle body are required so that the outer wheel paths can be measured. These extensions can be a safety hazard and make data collection difficult on high traffic pavements. Lasers capability of angular measurements have been used by some data collection equipment for these measurements. However, the lasers used are very expensive compared to the ultrasonic sensors and could be destroyed in an accident. There is a need for a less expensive laser displacement measurement system with resolution suitable for rut measurements. During this project a search was conducted to find less costly laser systems which would be suitable for transportation measurements purposes. When a suitable system was not found, a laser based measuring system was developed and investigated. This system is described in the report and could possibly be used as an alternative to the more expensive higher resolution systems.

BENEFITS

The successful completion of this project will not only provide a more accurate and quicker method of obtaining rutting information for the State, but will also provide a much safer method than is currently used.

PREFACE

This project report represents the final results from Project 1290. This project was initiated to develop a low cost laser displacement measurement system with a high degree of accuracy and resolution. This report discusses the results of the research.

This report was prepared in cooperation with the Texas Department of Transportation and the Federal Highway Administration, U. S. Department of Transportation. Special recognition is due to Carl Bertrand of the Texas Department of Transportation and Robert Harris formerly with the Texas Department of Transportation for supporting this research effort.

Roger S. Walker

October 1994

The contents of this report reflect the views of the authors, who are responsible for the facts and accuracy of the data presented herein. The contents do not necessarily reflect the official views or policies of the Federal Highway Administration. This report does not constitute a standard, specification, or regulation.

There was no invention or discovery conceived or first actually reduced in the course of or under this contract, including any art, method, process, machine, manufacture, design or composition of matter, or any new and useful improvement thereof, or any variety of plant which is or may be patentable under the patent laws of the United States of America or any foreign country.

CHAPTER ONE

Project Description

1.0 Introduction

This report provides findings and development documentation from Project 1290, Improved Rut Measurements methods for Siometers. Data from the Texas Department of Transportation's Pavement Evaluation System indicated an increase of rutting on Texas pavements. Rut measurements in Texas had consisted of Department personnel manually measuring the pavement surface. A low cost rut bar system was developed for automating this measurement process. Implementation of the system has begun on a regular bases for the annual data collection activities. This rut bar system uses the Siometer (R680) for data acquisition and the Polaroid ultrasonic measurement sensors for measuring rut distances.

In order to collect accurate rut data, which includes rutting generated by trucks, extensions outside the vehicle body are required so that the outer wheel paths can be measured. The extensions are required because the sensor must be mounted perpendicular to the measured surface in order to receive enough return signal for measurements. These extensions can be a safety hazard and make data collection difficult on high traffic pavements. Laser light has been used by some data collection equipment to alleviate this problem. However, the lasers used are very expensive compared to the ultrasonic sensors and could be destroyed in an accident.

With the increase in rutting seen in Texas over the last few years, a reliable rut measuring system has been needed. This project was initiated to perform several research tasks which would assist in developing a more reliable rut measuring system. Specifically, efforts were made to find more suitable sensors, and the development of better methodology for estimating rut depth from such sensor measurements. Additionally, during the project, after it became apparent that there were not any inexpensive alternatives to the expensive Selcom lasers, a lab laser was developed which might be used for such purposes. A phototype rut bar constructed in the Transportation Instrumentation Laboratory at UTA with the five acoustic sensors, was used for developing and/or implementing the various rut measurement algorithms.

This final report provides documentation on research efforts conducted in this project and which were not previously reported. The report is divided into four chapters including this one. Chapter 2, Laser Displacement System, provides details on the development of the UTA lab laser, which could possibility be used for rut measurements. Chapter Three, Piggyback Board, provides details on an interface board which will plug into the Texas Siometers or R680 units for interfacing with up to 8 analog signals or lasers. This board provides an expanded capability should lasers be used for rut measurements with the R680.

Chapter 4, Rut Measurement Procedures, describes the rutting algorithms and operating procedures developed during the project for the Texas DOT.

CHAPTER TWO

Laser Displacement System

2.1 Introduction

2.1.1 Background

Distance displacement measurements are used in transportation instrumentation for providing measurements from the vehicle frame or body to the pavement surface. These measurements are accomplished by either inexpensive acoustic devices or by more expensive and accurate laser systems. The acoustic devices have a tremendous cost advantage but are adversely effected by wind, texture, and moisture. The laser devices, if a strong enough laser is used, are not as effected by these conditions but are very costly. Acoustic devices also do not provide the same range of measurement resolution as the lasers. Current acoustic measurements for such purposes are only able to obtain around 0.05 inches of resolution, whereas laser systems can provide up to 0.004 or better inches of resolution. The Selcom laser, however, costs around \$11 to 15,000 where the acoustic system can be developed for under \$100.

There is a need for a less expensive laser displacement measurement system which could be used for rutting measurement procedures. During this project a search was conducted to find less costly laser systems which would be suitable for transportation measurements purposes. When a suitable system was not found, investigations were begun in the construction of a laser for this purpose. This chapter describes such a system.

2.1.2 System Description

Figure 1 illustrates how the laser light is emitted from a diode laser onto the surface of the object whose distance is to be measured. This light is then reflected back off of the surface. A portion of this light is focused using a converging lens onto a linear position sensitive detector (PSD). The location of the focused light on the PSD is determined by the laser detection circuit. This location can then be used to calculate the distance of the object. The location of the laser on the PSD is represented by the ± 10 volt output of the laser detection circuit. This analog signal is then digitized by an analog to digital converter and read by a Motorola 68332 microcontroller. The 68332 was used in the lab for the initial interface applications to control the functions of the A/D converter and performs statistical analysis on its output. If used with the R680, the analog signal would be directly connected to the Piggy Interface Board (Chapter 3).

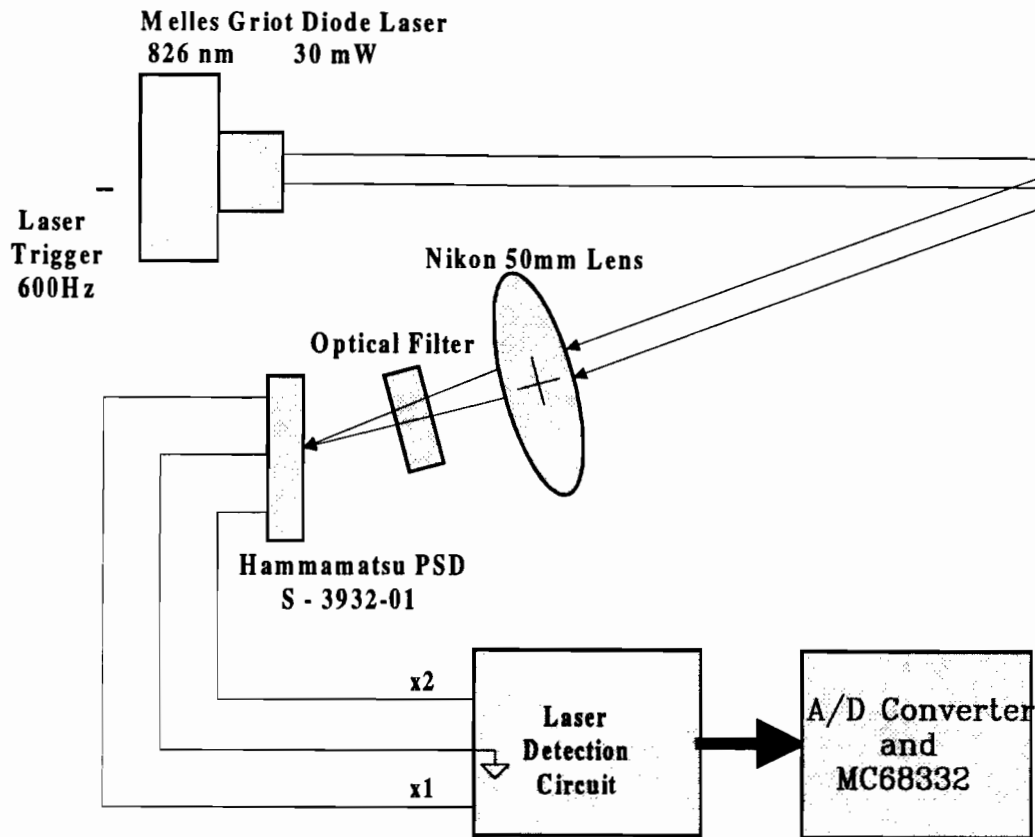


Figure 1. Laser Processing Method

2.1.3 System Requirements

The initial requirement was to design and build a low cost laser measurement system suitable for use for outside rut measurements. The range of measurement required is 8 inches (203.2mm). This range is centered around a distance of 15 inches (381.0mm) from the lens. The system should, therefore, be able to measure the distance from 11 inches (279.4mm) to 19 inches (482.6mm). The required resolution of the system is 1/20 of an inch (1.27mm).

2.2 Optical Triangulation

2.2.1 General Description

The approach used here to measure the displacement is possible because of a method called optical triangulation. Two common configurations use a spot of light or a line of light that is reflected off of a diffusive surface. The version of the method employed in Figure 2 uses a spot of light. The light spot is provided by a laser beam from a diode laser. The laser beam is directed such that it is incident normal to the diffusive surface. When the diffusive surface is displaced parallel to the laser beam, the spot of light on the surface will have a component of displacement perpendicular to the optical axis of the converging lens. This will result in a corresponding displacement of the focused light on the PSD. Since a

uses a spot of light. The light spot is provided by a laser beam from a diode laser. The laser beam is directed such that it is incident normal to the diffusive surface. When the diffusive surface is displaced parallel to the laser beam, the spot of light on the surface will have a component of displacement perpendicular to the optical axis of the converging lens. This will result in a corresponding displacement of the focused light on the PSD. Since a geometrical relationship exists between the object and its image, the displacement of the image on the PSD can then be used to calculate the displacement of the surface. This method is represented graphically in Figure 2.

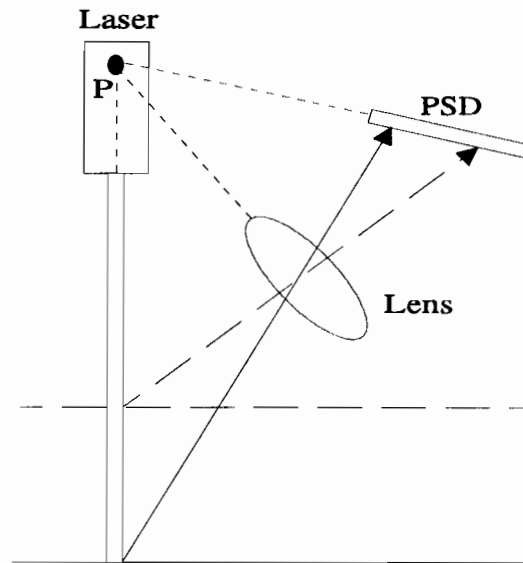


Figure 2. Optical Triangulation Process

2.2.2 Relationship Between Object Distance and Displacement

The basic geometry of the optical triangulation system shown above was designed in accordance with the Scheimpflug optical design condition. This condition states that the object plane, the plane of the lens, and the image plane should all intersect at a line. In this application, the condition indicates that to maintain the best focus of the laser beam spot on the detector that the laser beam, lens plane, and the plane of the detector must all intersect at a common point - point P.

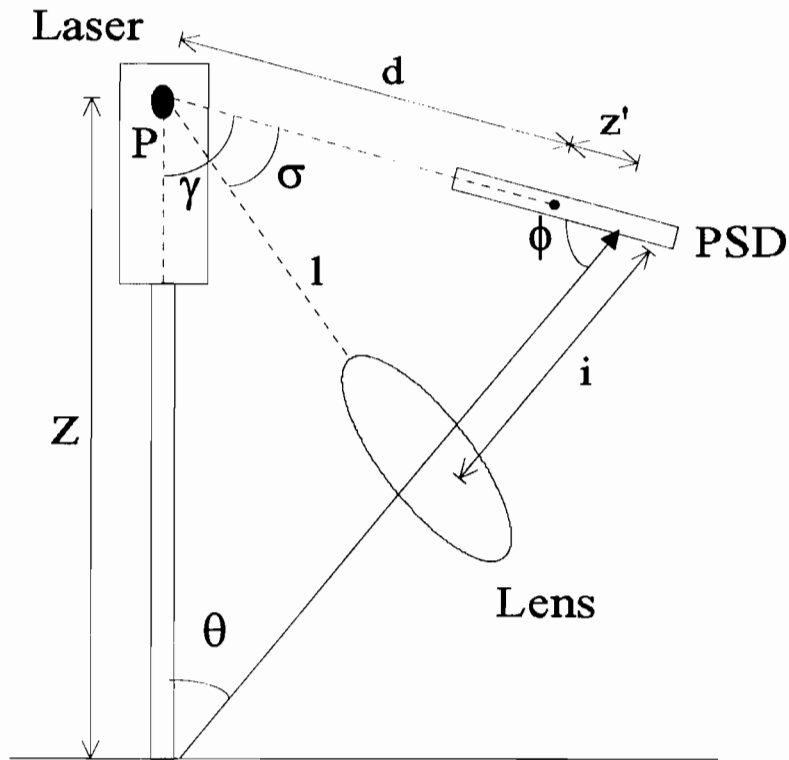


Figure 3. Optical Triangularization Relationships

Using Figure 3 above, a relationship can be derived between the displacement of the focused light on the PSD, $\Delta z'$, and the distance of the object Z . The position of light on the PSD, $\Delta z'$, is referenced to the center of the PSD. The total length of the PSD is 12 mm, therefore the value of $\Delta z'$ must be between -6mm and 6mm. Using the law of sines, the following relationship exists :

$$\frac{d + \Delta z'}{\sin \theta} = \frac{Z}{\sin \phi} \quad (1)$$

This is the governing equation relating Z and $\Delta z'$. The value of d in equation 1 is the distance from the point P to the center of the PSD. This value is constant and known. While the value of $\Delta z'$ is not constant, its immediate value will be provided by the laser detection circuit discussed later. Therefore, this value may be considered to be known as well. In order to solve this equation for Z , we must derive the values of θ and ϕ . To calculate ϕ , the law of sines is again used to obtain the following relationship:

$$\frac{\sin \phi}{l} = \frac{\sin \sigma}{i}$$

$$\sin \phi = \frac{l \sin \sigma}{i} \quad (2)$$

The value of l in equation 2 is the distance from the point P to the optical axis of the lens. This value of l is constant and known. Also known is σ , the angle between the PSD (line d) and the plane of the lens (line l), which is also constant. The value of i , the image distance, is not known and must be calculated. First, the equation can be solved for $\sin \phi$ and then plugged into equation 1 to obtain equation 1a:

$$\frac{d + \Delta z'}{\sin \theta} = \frac{Z \cdot i}{l \cdot \sin \sigma} \quad (1a)$$

In order to solve for Z , the values of i , the image distance, and θ must be calculated. The value of i is obtained by using the law of cosines to generate the following equation:

$$i = \sqrt{l^2 + (d + \Delta z')^2 - 2l(d + \Delta z') \cos \sigma} \quad (3)$$

The value of i may be immediately solved since the values of l , d , $\Delta z'$, and σ are already known.

Using the law of angles which states the sum of all angles of a triangle equals 180 and then solving for θ , the following equation is obtained :

$$\theta = 180 - \gamma - \phi \quad (4)$$

By substituting equations 3 and 4 into equation 1a, the following relationship between Z and $\Delta z'$ is derived involving only known values :

$$Z = \frac{(d + \Delta z') \cdot l \cdot \sin \sigma}{i \cdot \sin (180 - \gamma - \phi)} \quad (5)$$

2.2.3 Calculations of Angles and Distances Used

The Scheimpflug design condition discussed earlier provided the general framework for the optical system. The task remaining was to select the parameters d , l , σ , and γ such that the resulting system conformed to the specifications. In choosing the parameters, a tradeoff must be made between range and resolution. Within a narrow range a very high resolution may be obtained or very wide range of distances can be measured but with low resolution. In order to effectively test the infinite possible combinations of these parameters, the system was simulated in software. The simulator was based on the relationships

discussed in the previous section. The equations derived were implemented and various design configurations were tested before the actual system was built.

The first parameter to be selected was the distance, d , from point P to the PSD. This was arbitrarily assigned the value of 170 mm, based on previous experience with other devices. The value of σ was estimated based on the focal length of the lens and the initial assumption that the optical axis of the lens was to intersect the center of the PSD. Based on these values the initial value of σ and l were obtained. Since the maximum distance to be measured was 19 inches (482.6mm), as stated in the requirements, and the initial values of d , l , and σ had been calculated, an initial value of γ could be estimated. These initial values were used in the simulator and their results analyzed. Based on the mathematical relationships in the previous section and trial and error, the values were adjusted until the system performed as required. The final values for the parameters are as follows:

$$\begin{aligned}d &= 165\text{mm}, \\l &= 150 \text{ mm}, \\ \sigma &= 22.8^\circ , \\ \gamma &= 74.6^\circ .\end{aligned}$$

2.3 Optical Block

2.3.1 Diode Laser

The laser used is a Melles Griot 30 mW diode laser (model no. 06GIC108). The wavelength of the emitted light is 829 nm with a beam size of 1.0 x 3.33 mm. The output of the laser is collimated by passing it through a gradient index lens. This lens is included in the diode head assembly. The laser is powered by Melles Griot Series 300 Model 300/p laser diode driver. This is a low cost integrated laser driver assembly which is preset for a fixed laser output power. The output power of the driver was factory calibrated for this particular diode laser.

The laser on/off port (BNC connector) on the rear panel allows the power on and power off to be digitally modulated. A TTL signal applied here will modulate the laser output between being full off and full on. A TTL low corresponds to the laser being full on and a TTL high corresponds to the laser being full off. Shorting the on/off port results in the laser being in the full on state.

This system is designed such that the laser may be operated in the constant on, full power state, or modulated at a programmable frequency. The desired mode is determined by the position of a jumper on header J1 (see sheet 3 in Appendix A). Placing the jumper across J1:3 and J1:4 puts the laser in constant full power mode. If the jumper is across J1:1 and J1:2, the laser is toggled on and off at a frequency of 600Hz under control of the 68332 microcontroller. The frequency is provided by the pulse width modulation feature of the Time Processor Unit (TPU) on the 68332 and is fully programmable.

2.3.2 Optical Lens

The optical lens is responsible for collecting the reflected light from the surface and focusing it onto the PSD. Therefore, selection of the proper converging lens is crucial if the system is to perform to the desired specifications. There are three parameters which must be considered when selecting a lens. The first is the light gathering capacity of the lens. This capacity is proportional to its effective area or aperture. The aperture size is usually described in terms of its f-number. The f-number is defined as the focal length of the lens divided by the diameter of the lens. Because the light gathering capacity of the lens is proportional to its area and thus to the square of its diameter, changing the diameter by a factor of $\sqrt{2}$ corresponds to a factor of two in exposure. Therefore, the larger the diameter of a lens, the smaller the f/number and the greater the aperture and exposure. The lens chosen for this system has a focal length of 50mm with an aperture of f/1.4.

The light gathering capacity of the lens becomes more important as the reflectivity of the surface decreases. As the surface being measured becomes darker and more absorbent to the frequency of the projected light, less light will be reflected off of it and less light will be available to be focused onto the PSD. Therefore, a lens with a greater ability to capture the light that is reflected will be necessary.

The second parameter which must be considered is the focal length of the lens. The focal length is a physical property of lens. For the converging lens, it represents the distance from the lens where the light rays converge if the object distance is infinite. The relationship between object distance and image distance is represented graphically in Figure 4.

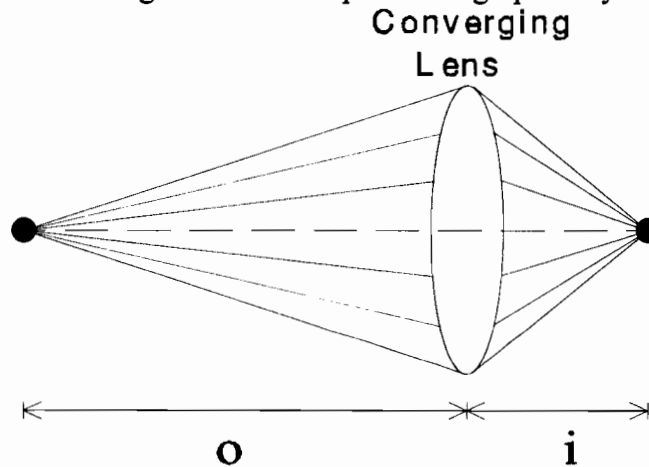


Figure 4. Relationship Between Object Distance and Image Distance

The equation which relates the focal length to the object and image distance is given by the following :

$$\frac{1}{O} + \frac{1}{i} = \frac{1}{f} \quad (6)$$

Relating this equation back to Figure 4, it can be seen that as the distance between the object and the lens (o) approaches infinity the $1/o$ term in the equation approaches 0. Therefore, the image distance becomes equal to the focal length. This, however, is not always the case. Depending on the range of distances to be measured and their proximity to the lens, the selection of a lens with an appropriate focal length becomes extremely important. For example, in this system it is necessary to measure distances anywhere from 480 mm to 280 mm from the lens. If a lens with a 120 mm focal length is used, the image distances would be the following :

object distance (o)	image distance (i)
480 mm	160.0 mm
430 mm	166.5 mm
380 mm	175.4 mm
330 mm	188.6 mm
280 mm	210.0 mm

The total difference in image distance is $210.0 - 160.0 = 50.0$ mm. The total length of the PSD used in this system is only 12 mm. Slight variations in image distance over a desired range may be overcome by angling the PSD in such a way that the end of the PSD which receives the larger image distance will be positioned further from the lens. Obviously, it would be impossible to maintain a focused beam on a 12 mm PSD with a variance of 50 mm in image distance, no matter how the PSD was angled.

By comparison, a lens with a 50 mm focal length over the same range would result in the following image distances :

object distance (o)	image distance (i)
480 mm	55.8 mm
430 mm	56.6 mm
380 mm	57.6 mm
330 mm	58.9 mm
280 mm	60.8 mm

Thus, the total difference in image distance across the desired range is $60.8 - 55.8 = 5$ mm. This difference is much more manageable by employing the method describe above.

The third parameter involved in lens selection is cost. As one approaches the ideal lens, which has maximum light collecting ability, the cost rises exponentially. The Canon 50 mm lens selected provides satisfactory light collecting ability at an acceptable cost

2.4 Position Sensitive Detector (PSD)

2.4.1 Structure and Specifications

The functionality of this entire system hinges on the ability to accurately measure the location of the focused light on a photosensitive device called a position sensitive detector or PSD. The PSD used in this system is the Hamamatsu S3932-01. The structure of this one dimensional PSD is visually represented in Figure 5. This device is composed of photosensitive material with electrodes attached at each end and a common node attached in the center. An effective capacitor is formed at the junction of the P-layer and N-layer. This "junction capacitance" is a major factor in determining the response speed of the PSD. This capacitance may be decreased by applying a bias voltage, V_r , to the common node of the PSD. This causes a decrease in the rise time of the output level thereby resulting in an increase in response speed of the PSD. The maximum voltage that may be applied before damage to the device occurs is 20 volts. This system allows the voltage to vary from 0V to 15V by adjusting the potentiometer R0.

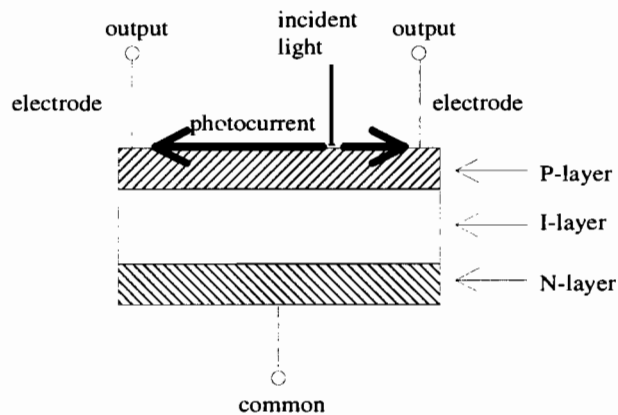


Figure 5. Hamamatsu S3932-01

The effective sensitive area is 1mm X 12mm. A visible cut resin window is provided which helps filter out all visible light and, thus, decreasing some of the noise introduced by light sources other than that of the laser. The visible cut resin window results in a spectral response of 700 to 1100 nm with the peak wavelength at 920 nm. This corresponds well with the 829 nm diode laser. The maximum resolution on the PSD is 0.3 μm and the interelectrode resistance is 5k Ω . The one dimensional PSD can be used for position detection of a laser beam with a minimum pulse width of 100 ps.

2.4.2 Theory of Operation

When the spot of light is focused onto the PSD, an electric charge is generated at the point of incidence which is proportional to the light energy. The PSD converts this electric charge into photocurrents I_1 and I_2 which flow from the spot of light toward the electrodes at each end. The relative magnitudes of I_1 and I_2 are dependent upon the position of the incident light. The conductive material of the PSD has a resistance associated with it. Therefore, the further the beam of light is from an electrode, the higher the resistance is between the spot of light and that electrode. This results in lower current flowing toward the

electrode. Conversely, the closer the spot of light is toward an electrode, the lower the resistance between the light spot and the electrode and the higher the current flowing to it.

If the spot of light falls on the middle of the PSD, the resistance between the spot of light and each of the two electrodes will be the same and equal currents will flow to each electrode. If the spot of light is closer to electrode 1 than electrode 2, then the current flowing toward electrode 1 (I_1) will be higher than the current flowing to electrode 2 (I_2). Using the ratio of these two currents, the exact location of the spot of light may be calculated. The following formula relates the photocurrents I_1 and I_2 to the position of the light spot:

$$\frac{I_2 - I_1}{I_1 + I_2} = \frac{2X}{L} \quad (7)$$

As shown in Figure 6, X is the distance from the center of the PSD to the spot of light and L is the total length of the PSD. Because the position is determined using a ratio of the two currents, it is independent of the strength of the incident light. This eliminates any variability which might be introduced due to changes in the strength of the spot of light focused onto the PSD caused by differences in the reflectivity of the surface being measured.

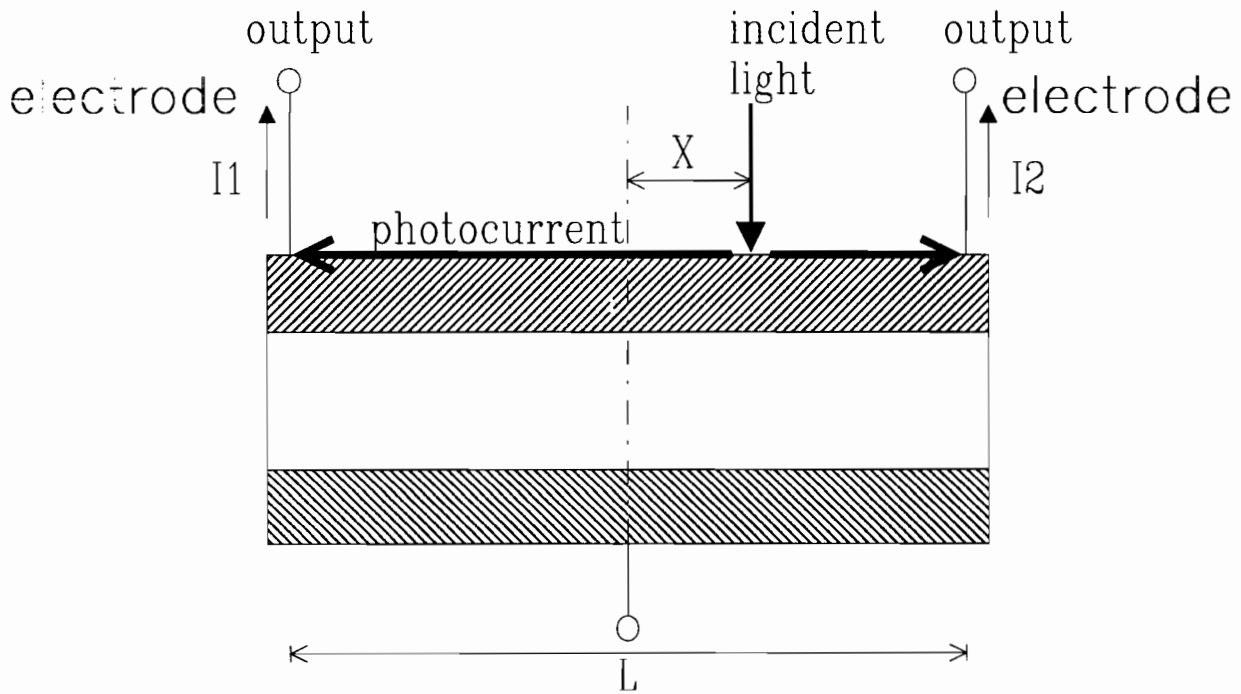


Figure 6. Hamamatsu Position Detector

2.5 Analog Position Detection Circuit

2.5.1 Stage 1 - Current to Voltage Conversion

The previous equation provided a relation between the currents I_1 , I_2 , and the position of the spot of light on the PSD. An analog circuit may be designed that implements the ratio of the sum and difference of equation 7. This circuit is shown in sheet 1 of Appendix A. The first stage of this circuit (U1:A and U1:B) uses current to voltage converters to transform currents I_1 and I_2 into voltages X_1 and X_2 . Feedback is provided through the parallel combination of a $100\text{k}\Omega$ resistor and a $.03\text{ pF}$ capacitor. By placing the capacitor in parallel to the resistor, any frequency above $1/(2\pi(100\text{k}\Omega)(.03\times 10^{-12}))=5\text{KHz}$ will be attenuated, thus functioning as a lowpass filter.

2.5.2 Stage 2 - Formulate Sum and Difference of Photocurrents

The second stages of this circuit produce the sum and difference of the voltages X_1 and X_2 . Op-amp U2:A receives X_1 and X_2 on the inverting input. Since both input resistors as well as the feedback resistor are all of the same value ($10\text{k}\Omega$), this acts as a summing amplifier with a gain of -1. The output of U2:A is equal to $-(X_1+X_2)$. This is then passed to U3:A which is just an inverting amplifier with a gain of -1. The output of U3:A is then (X_1+X_2) . U2:B receives X_2 on its non-inverting input and X_1 on its inverting input. All input and feedback resistors are of the same value. Op-amp U2:B, therefore, subtracts X_1 from X_2 giving X_2-X_1 .

2.5.3 Stage 3 - Calculating Ratios : Analog Division

Now that the sum and difference of X_1 and X_2 have been implemented, we must obtain their ratio. To do this an analog divider is used. The component selected for this design is the AD534 analog multiplier by Analog Devices. When configured, as shown by U4 in sheet 1 of Appendix A, it functions as an analog divider. The resulting transfer function for the divider is the following :

$$out = \frac{10V(Z_2 - Z_1)}{(W_1 - W_2)} + Y_1 \quad (8)$$

It receives the analog value of the numerator (X_2-X_1) as Z_1 on pin 11 and the analog value of the denominator (X_1+X_2) as W_2 on pin 2. Z_2 , W_1 and Y_1 are set to 0 by grounding the corresponding pins. Since the ratio X_2-X_1 to X_1+X_2 will always be between 1 and -1, the output of the analog divider will always be between ± 10 volts and proportional to the location of the position of the light spot on the PSD.

2.5.4 Stage 4 - Lowpass Filter

After the position signal has been generated, any high frequency components which might have been introduced must be removed from the position signal in order to increase the resolution and reliability of the signal. This is accomplished by using a first order lowpass filter that has a cutoff frequency of 5 KHz. The schematic for this filter is shown in sheet 2 Appendix A and the calculations of the component values are shown in Appendix B. Also, by

eliminating the frequencies above 5 KHz, the output of this filter may be sampled as low as 10 KHz without violating the sampling theorem.

2.5.5 Stage 5 - Band Reject Filter

When this system is used to find the distance of an object which is dark and light absorbent, the amount of reflected light focused onto the PSD may be quite small. If the system is used around a light source, such as fluorescent lights, which operate at 60 Hz, the true position signal from the laser must compete with the 60 Hz signal from the lights. This results in a signal which is the sum of the position signal and the oscillating 60 Hz noise.

To eliminate the 60 Hz component of the signal while leaving the components contributed by the true position signal, the output of the lowpass filter described above is passed through a band reject filter. The filter selected is a second order biquad band reject filter with $Q=6$. This filter will attenuate all component frequencies between 55 Hz and 65 Hz. Since the gain on this filter is -1, the output must be inverted by passing it through an inverting amplifier with a gain of -1. All equations and calculations of component values used are located in Appendix B, and the schematic is located in sheet 2 of Appendix A.

2.6 Test Results

Preliminary tests were run on several different types of surfaces for various ranges. From these tests, resolutions better than 0.5 mm have generally been found. One advantage of the above design is that different ranges and offsets can be specified. Some typical results are illustrated in Appendix C for asphalt and plain white paper target samples.

CHAPTER THREE

Piggy Back Board

3.1 Introduction

The R680, currently used by Texas State Department of Transportation, was originally developed for measurement of road roughness by providing an estimate of profile and a measure of serviceability index. The profile was estimated by only using inputs from an accelerometer and distance sensor. The device used these two inputs to provide a statistical model of the vehicle in which it was installed. This modes was then used to eliminate the influence of the vehicle when making road measurements. Since, the system has been upgraded to accommodate the capability for measuring profile using the South Dakota method and for measuring rut via acoustic sensors.

As noted in Chapter One, extensions to the rut bar are used for measuring rutting caused by trucks. Without such extension, a laser distance measuring system capable of angle measurements is needed. In order to accommodate such lasers, the R680 units owned by the Texas DOT would require major changes. Thus to reduce these changes, a separate board was designed which could fit onto to the R680 board and provide this expanded interface. This board was named the Piggy Back Board (PBB) as it fits 'piggy back' over one of the IC sockets. This chapter describes the board.

3.2 Overview

The PPB allows for both multiple analog input signals and digital input/output signals. The board includes two MC68230 PIT ICs. One simply replaces the functions performed by the original R680 PIT. The other provides an interface to the eight channel A/D converter and also additional parallel lines for communications with other sensors and processors.

3.2.1 Original A/D and PI/T (68230)

The interface of the PIT and single channel A/D converter on the original R680 (R680C) is illustrated in figure 7. The PBB will provide this same PIT interface, an additional PIT for future parallel interface, and an eight channel A/D converter.

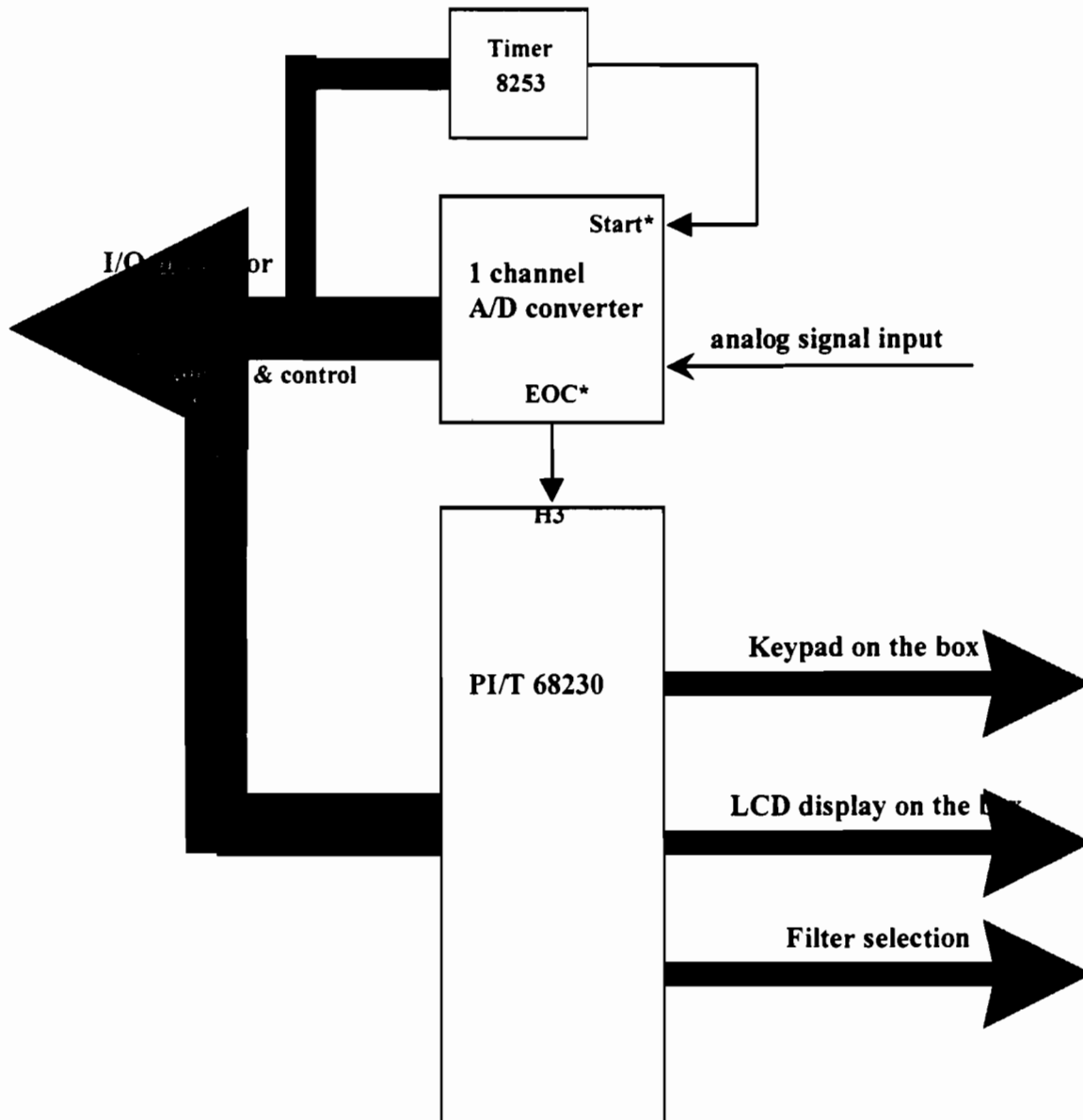


Figure 7. Original A/D and PI/T (68230) on the R680

3.2.2 R680 with the Piggy Back Board Addition

Figure 8 provides a functional block diagram of the PBB which replaces the original 68230 and single channel A/D converter shown in figure 7. The board includes socket pins which will fit directly over the socket which held the original 68230. Eight additional pins above the socket are also used.

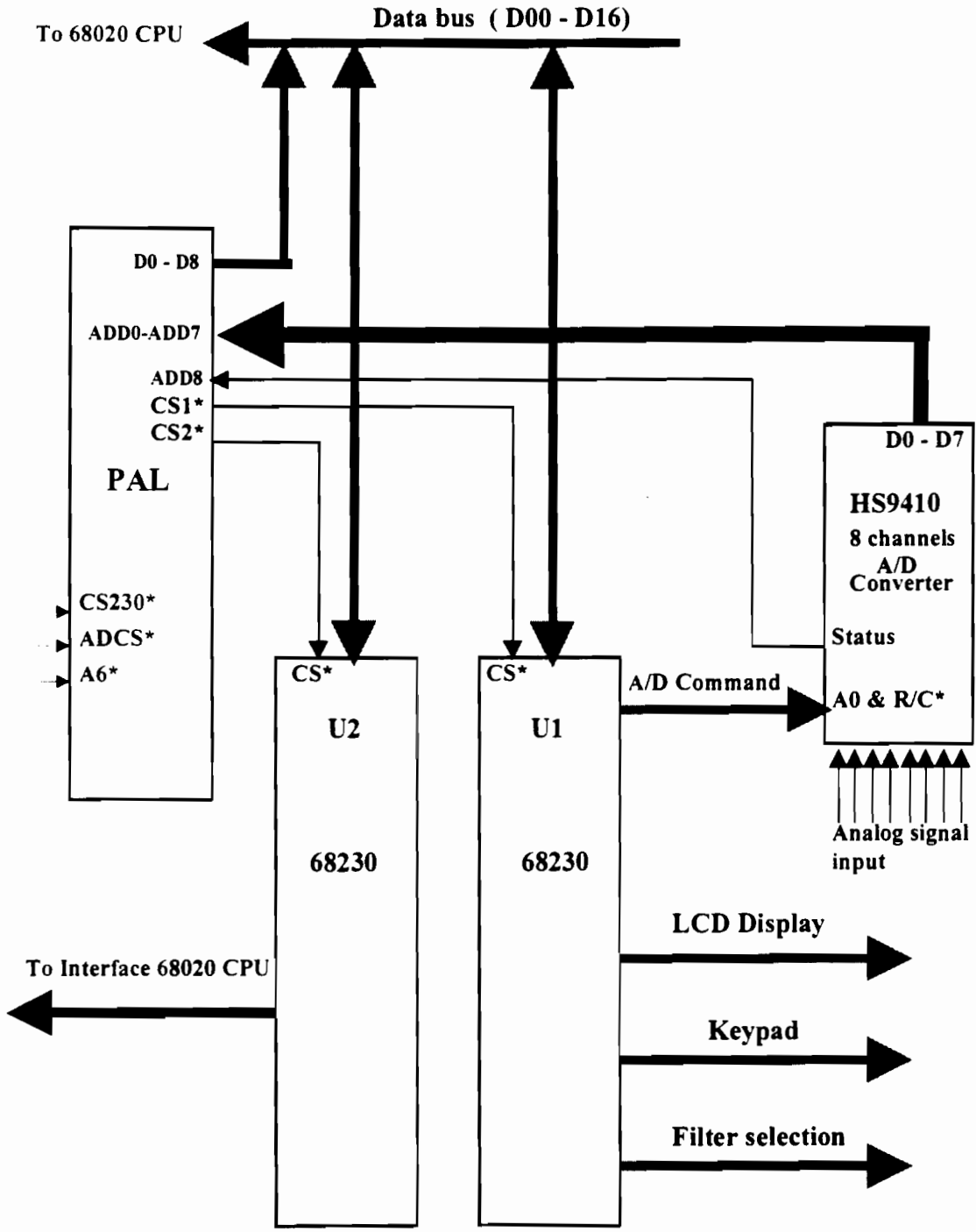


Figure 8. Piggy Back Board

3.3 Specific Descriptions of the Piggy Back Board

3.3.1 Memory Map

Figure 9 displays the memory map input/output for the 68230 and the A/D converter.

Device Type	Description	Address Range
U1 68230 PI/T	68230 PI/T (32 Bytes)	\$ 0001:0001 - - - - - \$ 0001:0020
U2 68230 PI/T	68230 PI/T (32 Bytes)	\$ 0001:0041 - - - - - \$ 0001:0060
HS 9410		\$ 0001:8000

Figure 9. Piggy Back Board Memory Map

3.3.2 Pal (P22V10)

In the Piggy Back Board, the PAL chip provides address decoding and A/D buffers. Figure 10 illustrates the PAL's pin assignments.

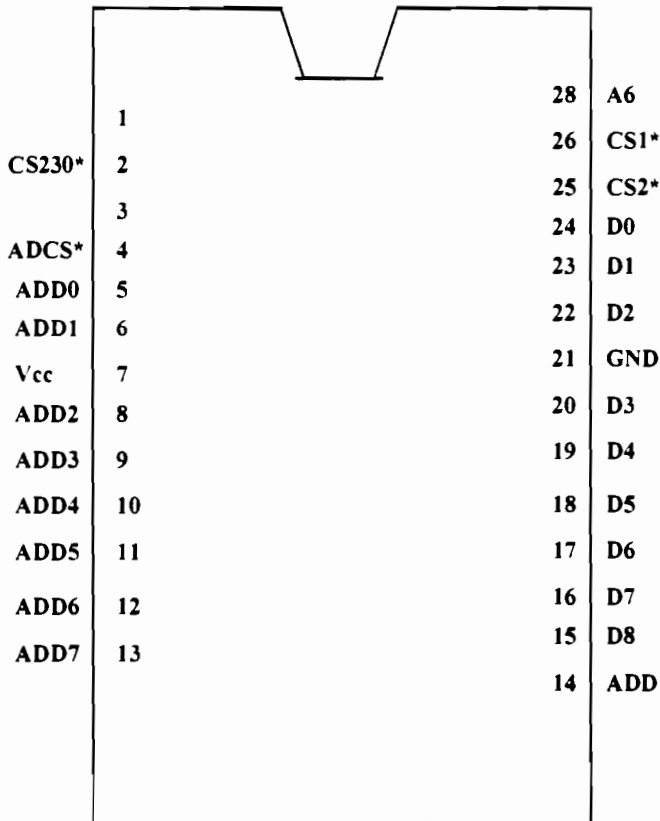


Figure 10. PAL (P22V10) Pin Assignment

3.3.3 PAL Equation

The below AMD PAL equations defines the internal functions of the PAL.

PALASM Design Description

----- Declaration Segment -----

```
TITLE PIGGY230 BOARD PAL
PATTERN 1
REVISION 1A
AUTHOR Brian Burgess
COMPANY UTA
DATE 05/06/92
```

CHIP PIGGY230 PALCE26V12H

----- PIN Declarations -----

```
PIN 2 /CS230 COMBINATORIAL ; INPUT
PIN 4 /ADCS COMBINATORIAL ; INPUT
PIN 5..6,8..14 ADD[0..8] COMBINATORIAL ; A/D converter Data OUTPUT
PIN 7 VCC
PIN 15..20,22..24 D[8..0] COMBINATORIAL ; OUTPUT
PIN 21 GND
PIN 25 /CS2 COMBINATORIAL ; OUTPUT
PIN 26 /CS1 COMBINATORIAL ; OUTPUT
PIN 28 A6 COMBINATORIAL ; INPUT
```

----- Boolean Equation Segment -----

```
EQUATIONS
D[0..8]=ADD[0..8]
D[0..8].TRST=ADCS
CS1=CS230*/A6
CS2=CS230*A6
```

----- Simulation Segment -----

```
SIMULATION
TRACE_ON ADD[0..8] D[0..8] A6 /CS230 /CS1 /CS2 /ADCS
SETF /ADCS
SETF ADD[8,7,6,1,0] /ADD[5,4,3,2]
SETF ADCS
SETF /ADCS
SETF CS230 /A6
SETF /CS230
SETF CS230 A6
SETF /CS230
TRACE_OFF
```

3.3.4 Running Mode for the HS 9410 A/D Converter.

The HS 9410 A/D converter has two operating modes. The first mode is for A/D conversion. It will send out either 8 bits or 12 bits of data to the host using only 8 data output pins. The second operating mode is for interface with the data bus.

Some general comments should be noted regarding the A/D operation:

- System 8 bits data lines (D00-D07) are used to connect with HS 9410 A/D converter 8 bits data pins. The S9410 status pin (which indicates whether or not the conversion is completed) is connected to the D08 line of the system data bus.

- The Running Procedure:
 1. Use 68230 to send the start conversion command to the HS9410.
 2. HS9410 begins the conversion and sets the status pin to 1. Since the status bit is connected to D08 line, the data is read from the A/D converter address (\$ 18000) and bit 8 checked to see if the conversion is complete. (If the bit 8 is 0, the conversion is completed, and the data is ready to be read.)
 3. Because there are only 8 data lines, the data is read twice. The first time the MSB 8 bits of the 12 bits data are read. The second time is LSB 4 bits of the 12 bits data in the upper nibble byte and with 4 0's in the lower nibble byte. So, the data needs to be shifted and combined to get the 12 data bits.

- Figure 11 is the Flow chart for the above list of running procedures.

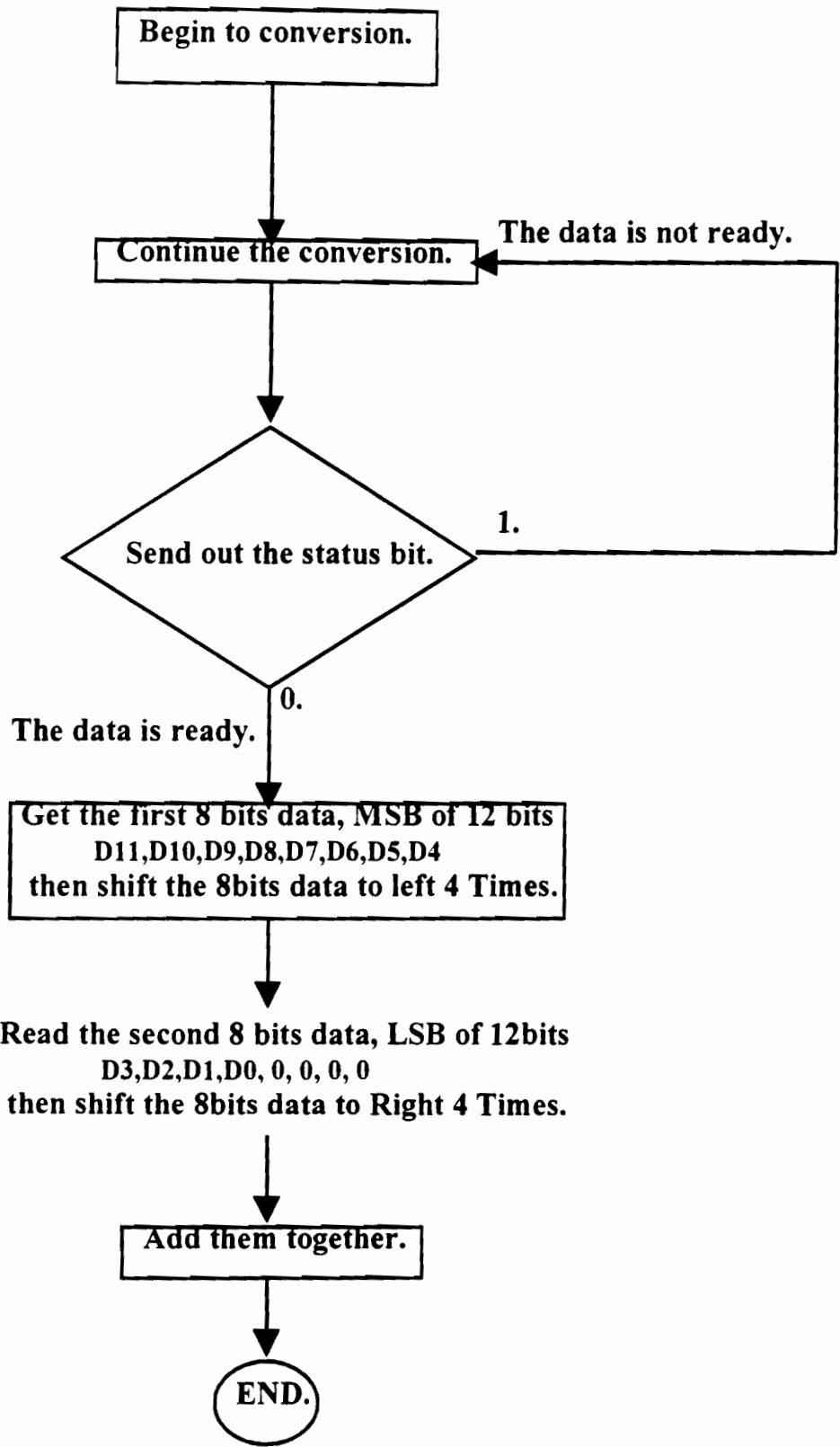


Figure 11. Flow Chart for Programming A/D Converter

CHAPTER FOUR

Rut Measurement Procedures

4.1 Introduction

This chapter provides a description of the rut bar procedures developed during the project for the Texas DOT. An automated rutting system is being used for measuring network level rutting. The methods used prior for rutting methods involved manual procedures which were inconsistent, time-consuming and dangerous. The Texas automated rutting system is based around the R680. Recent versions of the R680 (R680D) included rutting procedural capabilities. Many of the older R680 (R680C) have been upgraded to also include rutting procedural capabilities so that these devices can also be used for rut measurements.

The rutting procedures discussed are based on five ultrasonic or acoustic sensors placed on the front of an automobile. The development of these methods were facilitated by the use of the rut bar prototype in the University of Texas at Arlington Instrumentation Laboratory. Figure 12 illustrates the placement of the five acoustic sensors on the rut bar. The Texas DOT has developed rut bars for each of the vans used for rut and roughness measurements.

Three rut measurement methods are used by the Texas DOT and are subsequently described. A project level rut bar, which can include more rut measuring sensors (either laser or acoustic), can optionally use a fourth method. In the automated rut measuring system, the distance sensors are used to obtain a representation of the cross section of the road.

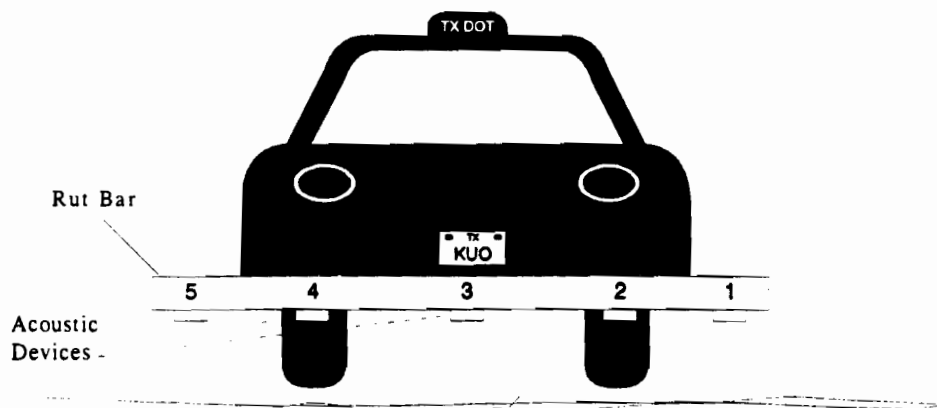
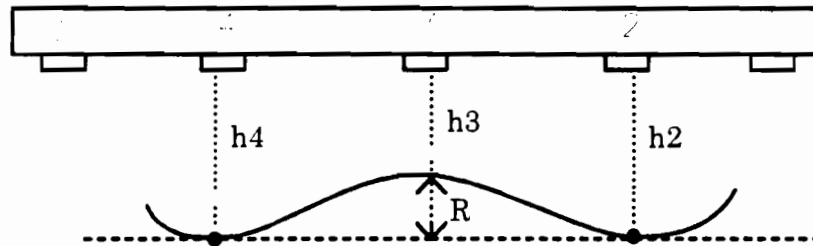


Figure 12. Texas Five System Rut Bar

4.2 Rut Measurement Methods

4.2.1. South Dakota Method

The South Dakota Rutting method was first introduced and implemented by the South Dakota DOT on their profiler. For this method, three acoustic sensors are used for measuring the differences between the center and right and left wheel paths as illustrated in Figure 15. Note that acoustic #3 is above the center of the lane, #2 is above the left wheel path, and #4 is above the right wheel path. The term (h_2-h_3) defines the rut at the left wheel path. Similarly, (h_3-h_4) defines the rut at the right wheel path. The average of the two ruts $(h_2-2h_3+h_4)/2$ is the South Dakota formula of ruts. There is no rut if the result is negative.



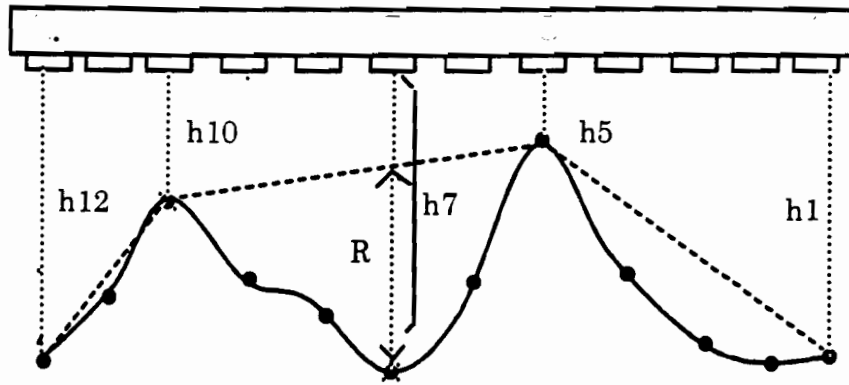
$$R = (h_2 - 2h_3 + h_4) / 2$$

Figure 13. South Dakota Method

4.2.2. String Line General

The remaining rut methods may be considered variations of the general string line procedure which is illustrated in Figure 14. This general method is outlined as follows:

If we lay a hypothetical string along the cross section of the surface of the road, all the straight or convex portions of the road will contact the string, and all the concave portions of the cross section, the ruts, will be under the string. The position of the deepest rut is found where the surface of the road is farthest from the string. This maximum depth is defined as the rut depth of the cross section. Practically, we use distance sensors to measure the depths of a number of nodes on the cross section with respect to a horizontal rutbar. The measured cross section of the pavement is simplified to a polyline. The hypothetical string also becomes a polyline. Thus the nodes on the cross-section polyline that do not touch the string are the rut candidates. We developed an algorithm for the computer to construct this string and find the nodes that are ruts.

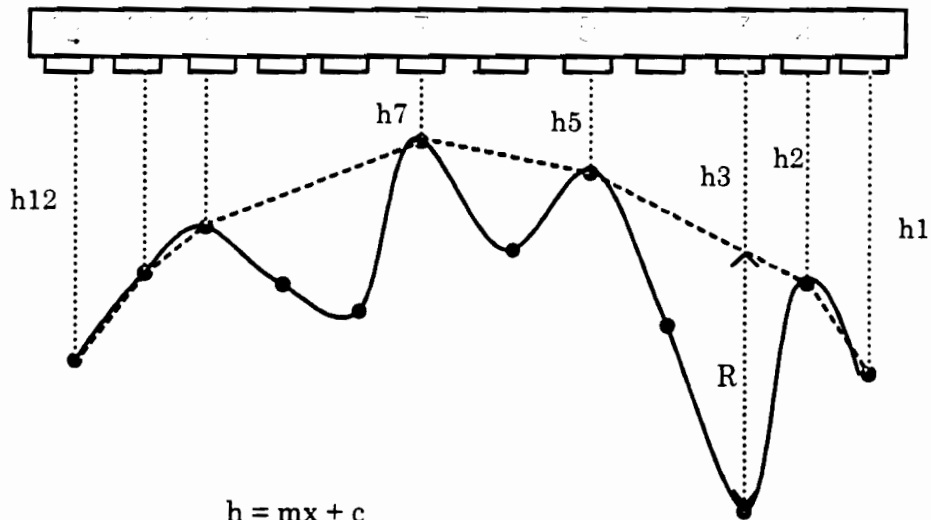


$$h = m * x + c$$

$$m \text{ (slope)} = (h_{10} - h_5) / (x_{10} - x_5)$$

$$c = h_{10} - (m * x_{10})$$

$$R = h_7 - (m * x_7 + c)$$



$$h = mx + c$$

$$m \text{ (slope)} = (h_5 - h_2) / (x_5 - x_2)$$

$$c = h_5 - (m * x_5)$$

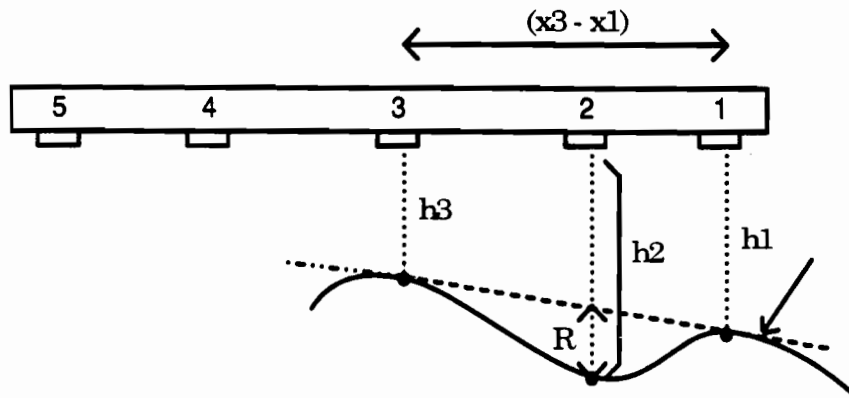
$$R = h_3 - (m * x_3 + c)$$

Figure 14. String Line General

The general method is illustrated for the two cases above.

4.2.3. String Line Left Method

The String Line Left Method is a simplified case of the String Line General Method in which only three distance sensors, acoustic devices #1, #2, #3, are used. Device #3 is above the center of the lane, device #1 is above at the left edge of the lane, and #2 is right above the left wheel path.



$$h = mx + c$$

$$m \text{ (slope)} = (h_3 - h_1) / (x_3 - x_1)$$

$$c = h_3 - (m * x_3)$$

$$R = h_2 - (m * x_2 + c)$$

Figure 15. String Line Left Method

4.2.4. String Line Right Method

The String Line Right Method is similar to the String Line Left except that it measures the rut at the right wheel path.

4.2.5. Absolute Right Method

Because of problems with drop off of pavements along the roads with no shoulders, Carl Bertrand of the Design Division-Pavements Section of the TxDOT suggested a modified method, which will be called the Absolute Right Method. For this method a rut is defined as the depth of the right wheel path with respect to the center of the lane. If the term $(h_4 - h_3)$ evaluates to a negative number or zero, it is considered no rut.

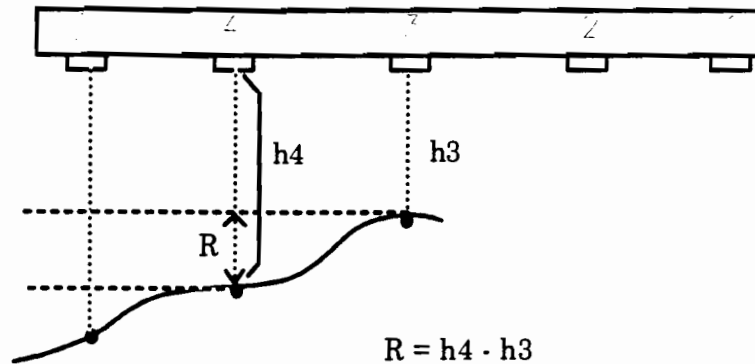


Figure 16. Absolute Right Method

4.3 Rut Measurement Procedures

4.3.1 Overview

When collecting real-time SI (Serviceability index) and rut, the R680 reads the five ultrasonic/acoustic devices attached to the front of the vehicle and sends the readings, the SI values, and the measurement speeds to the serial port. A communication program, TALK80.EXE, running on the PC receives the SI and the acoustic data and stores the raw data and/or the computed rut data. TALK80 can be set up to interface with the Mission Manager system, a video system being developed by the Texas DOT for the multifunction vehicle (MFV). When running under the Mission Manager system, it receives the start-data-collection command from the Mission Manager system and sends distance signals and computed ride and rut data to the system as the data is collected.

The program RUTBAR1.EXE lets the user select raw data files, output options, rut calculation methods, and section length storing these options in a temporary file. The program RUTBAR2 reads these options and produces the rut report file RUT.DAT, the SI report file RIDE.DAT, and ACOUSTIC.DAT which can be used by the Graphical Rut Analysis Program. The RUT.DAT and RIDE.DAT files can be input into the TxDOT PMIS database.

4.3.2 Initialization

The syntax of running TALK80 under DOS is:

TALK80 <optional initialization file>

The initialization file is required if real-time rut computation is selected. The initialization is a text file, and each entry is one line. The file name is assumed TALK.INI in this document.

The syntax for each entry is:

keyword = value list [optional comment]

The keywords are not case-sensitive. The value list can be a value or multiple values. Spaces before the keyword and spaces between the equal sign and the first value are acceptable. Comments can be entered after the value list as long as they are separated by at least one space.

There must be at least one space between two values if multiple values are entered. The program ignores lines that do not start with a valid keyword. Also, the program will not detect multiple entries with the same keywords; the last entry will override the previous ones.

Figure 17 is a sample initialization file. Most of the keywords are self-explanatory. A short comment is given at the end of each entry. The longer comments, which have an '*' on the first column, are given in separate lines. Note, detailed explanations of some keywords are given after Figure 19. In this document, the acoustic devices are numbered from one to five with number one being the first from the driver's side. Sometimes it may be required that data is entered for the acoustic devices in this order.

```

*The following entries are optional and can be entered later when
*TALK80 is running. You save time by entering them in this file.

COLLECTMODE = 3           Sets data collection mode to mode 3
header = select.hdr.     Header is stored in SELECT.HDR
acoustic = 12345         Selects all acoustic devices
fps = 4                  Samples acoustic data every 4 feet
gen_filename = Y        TALK80 generates name for raw data
files
comment = N              Do not prompt for comments
F5 = N                   F5 (mode changing is disabled.
F2 = N                   F2 (changing of communication
                        parameters) is disabled.

*The following entries are essential to real time rut data collection.

AC_SPACING = 24.0 36.0 36.0 24.0
RUT_SEC_LEN = 528      Rut report interval is 528 ft.
RUT_RANGE = 0.5 1.0 3.0
RUT_CORR = -2.07 -1.34 0 0.2 0.5          acoustic #I - acoustic #3
COM3IRQ = 2             use IRQ2 for COM3
RUT_METHOD = 12         New Average (String-Line Left & Right Rut)

*RUT_METHOD tells TALK80 which rut method to use. Pick a number from the
*following.
* 0: Do not do real time rut
* 1: South Dakota
* 2: String-Line Right
* 4: String-Line Left
* 6: String-Line Right & Left
* 8: Right Rut
*12: New Average (String-Line Left & right Rut)
* Use 0 if no real-time rut is needed. Add 16 to the number if you plan
* to interface with the video system

```

Figure 17. Sample Initialization File

The parameters in this file are as follows:

AC_SPACING specifies the distances between acoustic #1 and #2, #2 and #3, etc. The unit is inch.

RUT_SEC_LEN specifies the rut report interval in feet. The options are 528 feet and 1056 feet.

RUT_RANGE sets up the brackets for the three rut levels in the report. The three numbers (r1, r2, r3) are depths of rut in inches. They tell the program to calculate percentages for ruts in three ranges:

1. $r1 \leq \text{rut} < r2,$
2. $r2 \leq \text{rut} < r3,$
3. $\text{rut} \geq r3.$

The report format was changed from three levels to two in January, 1993, therefore the third value is currently optional.

RUT_CORR specifies the mounting offsets of the five acoustic devices in inches. Ideally, all the acoustic devices should give the same reading if the rut bar is over a level reference surface (water trough). They don't, because the rut bar may not be perfectly horizontal on the vehicle and the acoustic devices may have different stand-offs on the rut bar. We want to find the correction for this situation. The mounting offset of each acoustic device is defined as the reading of that acoustic device minus the reading of the #3 acoustic device (center one) in inches when the vehicle is unloaded and the rut bar is over a horizontal surface. Enter those five offsets in inches. The readings of all acoustic data can be obtained by using TALK80 with the Siometer running in Monitor Mode. Press F7 to perform a test which will give 20 readings of each acoustic device and 20 readings of the accelerometer. Use the average of 20 readings for accuracy. Let w1, w2, ..., w5 be the average readings (in inches) of the corresponding acoustic devices. The mounting corrections c1, c2, ..., c5 are:

$$c1 = w1 - w3$$

$$c2 = w2 - w3$$

$$c3 = w3 - w3 = 0$$

$$c4 = w4 - w3$$

$$c5 = w5 - w3$$

Enter in the initialization file:

$$\text{RUT_CORR} = c1 \ c2 \ c3 \ c4 \ c5$$

The keyword RUT_METHOD specifies the rut method for the real-time rut computation. A complete list of options is in the example file. The real-time rut computation is disabled when it is set to zero. Note that if you want to interface the rut system with the video system, you need to add 16 to the RUT_METHOD. For example, by using 28, you tell TALK80 to use RUT_METHOD 12 (string-line-left and right rut) and to communicate with the video system.

The keyword COM3IRQ specifies the IRQ number for COM3. COM3IRQ needs to be set up if you want to interface with the video system in which case three serial ports (COM1, COM2, and COM3) are used at the same time. The program assumes that COM1 uses IRQ4, and that COM2 uses IRQ3. You can use IRQ2 or IRQ5 for COM3. This option is only useful when RUT_METHOD is greater than 16.

4.3.3 Loading Correction and Procedure

The rut calculation assumes that the rut bar stays horizontal all the time. It is important to note that the mounting correction does not correct the situation where the rut bar changes its inclination from the loading condition, road surface, and responses of the vehicle's tires and suspension system.

Ideally, the rut bar's inclination should be known at the exact time of the acoustic data sampling. Then, it would be possible to correct the acoustic readings so that they matched the condition where the rut bar was horizontal. A precise way to obtain the accurate inclination at the time of the sampling is by use of a gyroscope on the rut bar. There is no gyroscope installed in the current systems. The following steps correct the inclination that results from different loading conditions:

1. Run TALK80 with the Siometer. Make sure the Siometer is in the Time mode and Monitor Mode.
2. Press SHIFT-F7 to initiate the calibration procedure. The program will display the mounting correction values and the previous loading correction values in inches. The program also prompts:

Press [F7] to do the UNLOADED condition.

(You may press [ESC] to abort the function.)

3. Unload the vehicle - the driver and all other occupants get out of the vehicle. Press F7 to collect the acoustic readings for the unloaded condition. The program will come back with the five displacements in inches for each of the sensors. Each value is the average of 20 acoustic readings. The program then prompts

[ESC] -Abort [F6] -Repeat [F7] -Accept

Press F6 to repeat the process or press [ESC] to cancel the procedure if you're not satisfied with the result.

4. Press [F7] to accept the displacements for the unloaded condition. The program will prompt:

Press [F7] to do the LOADED condition.

5. The driver and other vehicle occupants need to get in the vehicle before pressing [F7]. Similar to step 3 and 4, you can abort the function, repeat the sampling, or accept result.

6. If the readings for the loaded condition are acceptable, the program calculates the loading corrections as follows:

$$C_i = L_i - U_i \\ i = 1, 5$$

where c_1 - c_5 are the corrections, U_1 - U_5 the unloaded displacements, and L_1 - L_5 loaded displacements. The loading corrections will be saved in the file RUTCORR.INI. The loading corrections are then added to the mounting corrections and multiplied by the counts per inch of the acoustic devices (20) to give the total corrections in terms of acoustic counts.

4.3.4 Data Collection

The following procedures give step-by-step instructions on how the data should be obtained.

1. Connect the PC to the Siometer via serial ports. If the Mission Manager system is used, connect the Siometer serial port to COM1, connect COM2 to the command channel and COM3 to the DMI channel. If the Mission Manager system is not connected, use either COM1 or COM2 for the Siometer.
2. Run INI20.EXE to set up parameters in the Siometer if the current values of those parameters are unknown.
3. Make sure the initialization file for TALK80 is set up properly.
4. Run the header selection program.
5. Run TALK80.EXE with the initialization file.
6. Press F9 to start data collection. If the initialization file is not used, the user must make sure the baud rate is correct and the data collection mode is mode 3.
7. Enter the following information at the prompt. Some of them may not appear if they have been set up in the initialization file.
 - a. Output file: Enter file name and hit RETURN to continue or hit RETURN with empty file name to abort function.
 - b. Enter two lines of comment: If header is specified in TALK.INI, the header will be used for the first line of comment (only the second line of comment is asked). If "comment = N" is specified, no comment is asked.
 - c. Enter selected acoustic devices: Acoustic devices are numbered 1-5 from left to right. Type 12345 to select all. Type 1234 to select 1,2,3,4, etc. The acoustic devices selected must be suitable for the desired rut method.

- d. Enter distance between samples in feet (enter an integer). One sample every four feet at fifty miles per hours is the current setup. Be aware that there is a limit to the sampling rate the system can run.
 - e. Enter distance: You can enter the distance in feet by entering a number followed by an 'F' (or 'f'), or in miles by entering a number followed by an 'M' (or 'm').
8. The program will prompt "Hit any key to start running SI." Hit any key to start data collection when the vehicle reaches the beginning of the section of interest.
 9. While data collection is in session, you may hit a number from 0 to 9 to mark Pavement Management Information System (PMIS) comment code(s) of that section. The number will be displayed on the screen until the next section starts and will be written to the report file. You may also hit 'C' or 'c' (originally for Concrete) to suppress the rut report temporarily until you hit another 'C' or 'c' to resume rut report.
 10. Normal data collection terminates when the target distance is reached. Data will be saved automatically. The user can terminate at any time by pressing <ESC>, in which case the program will ask whether the data file is to be saved. Enter "Y" or "N." The program will save or discard the RAW data file accordingly. The SI data file (currently RTRIDE.DAT) and rut report file (currently RTRUT.DAT) will be saved regardless.

4.3.5 Post Processing

1. Run RUTBAR1. A list of all the files in the current directory will be shown in a box.
 - a. Select the data files by using the arrow keys to move the highlight bar to the file names and pressing the space bar. A selected file can be dropped by pressing the space bar again.
 - b. Press F10 to confirm the selection or press ESCAPE to abort the program.
 - c. Select one to three from the following three output files: RUT.DAT(rut report), RIDE.DAT(SI and speed), ACOUSTIC.DAT (used by the graphical rut analysis program).
 - d. Select one rut method from the six listed methods.
 - e. Select section length for rut reporting. It's either 0.1 mile or 0.2 mile.
 - f. A file named FILELIST.*** which contains the selected options and the file name will be generated and used by RUTBAR2.
2. Run RUTBAR2. Outputs will be APPENDED to the RUT.DAT, RIDE.DAT, and ACOUSTIC.DAT.

CHAPTER FIVE

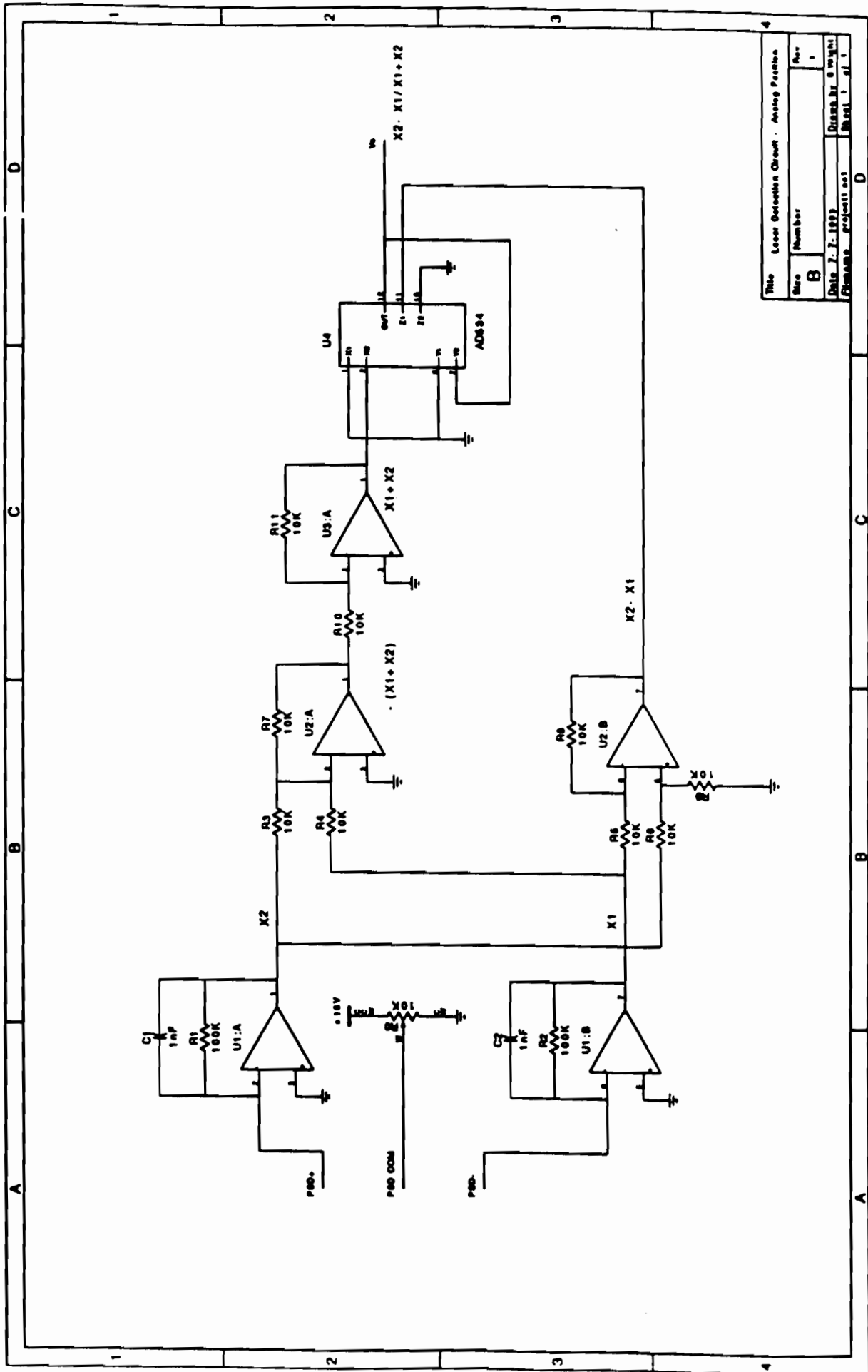
Conclusions

As discussed in Chapter 1, a reliable rut measuring system is needed for rut measurements in Texas. This project has provided research for methods which would enhance the development of such a system. In particular, better reporting procedures were developed and implemented. A prototype rut bar constructed in the Transportation Instrumentation Laboratory at UTA with the five acoustic sensors was used for developing and/or implementing the various rut measurement algorithms.

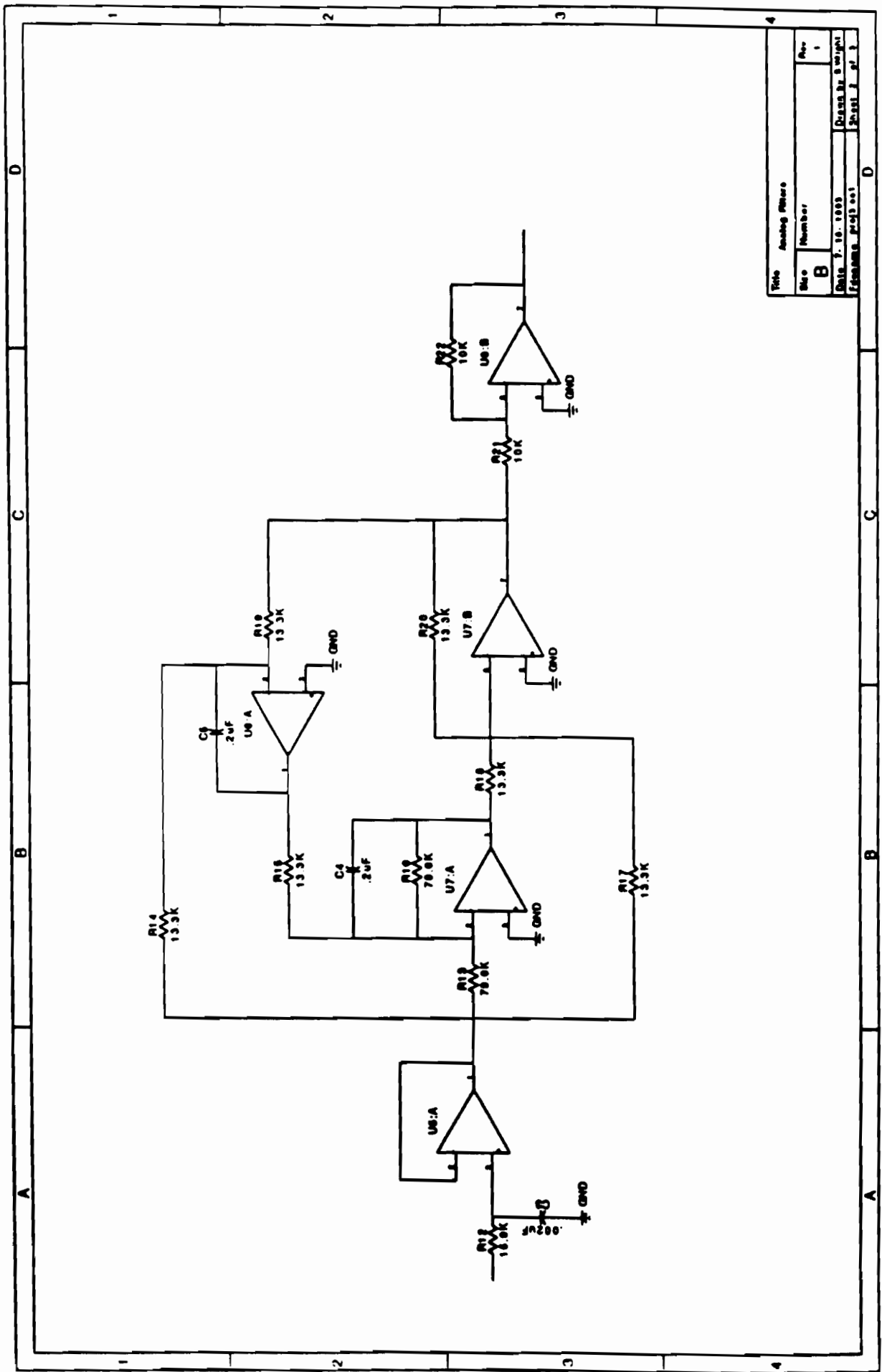
An objective of the project was to determine if an expensive laser could be used for rut measurements and, in particular, for measuring rutting outside of the vehicles bumper. After it became apparent that there were not any inexpensive alternatives to the expensive Selcom lasers, a lab laser was developed which might be used for such purposes. A complete description of this laser is provided. This information could be useful for building such sensors. An interface was designed for the roughness measurements used by the TxDOT if additional analog channels were desired.

The rutting procedures developed are presently being implemented by the TxDOT using the acoustic sensors. These sensors are currently the most inexpensive method of getting rut information, however, they have a number of undesirable characteristics. Lasers or some other type of infra-red light system that would enhance the measurement process are too expensive. Some states and manufacturers, however, are using such sensors for rut and transverse profile measurements. It is recommended that Texas continue the use of the acoustics, but may later want to build or obtain a rut bar with lasers or the combination of acoustics and lasers for such measurements. The procedures developed in the report could be adapted to such sensors.

Appendix A : Schematics for Laser Displacement System



Title		Leonor Geronimo Ochoa - Analog Feedback	
Size	Number	Rev.	
B		1	
Date		7-7-1993	
Filename		proj011.asi	
Sheet		1 of 1	



Title	Analog Filter
Size	Number
B	1
Date	7. 10. 2003
Filename	Proj3.ees
Sheet	1 of 1

Appendix B : Filter Design

1. First Order Lowpass Filter with Cutoff Frequency of 5 KHz

$$C = \frac{10}{f_c} = \frac{10}{5 \times 10^3} = .002 \mu F$$

$$R = \frac{1}{b\omega_c C} = \frac{1}{(1)(2\pi)(.002 \times 10^{-6})} = 15.9 K\Omega$$

Second Order Biquad Band Reject Filter with Center Frequency of 60 Hz

$$f_u = 65 \text{ Hz}$$

$$f_l = 55 \text{ Hz}$$

$$B = 65 - 55 = 10 \text{ Hz}$$

$$f_o = 60 \text{ Hz}; \omega_o = 376.99 \text{ rad/s}$$

$$Q = \frac{f_o}{B} = \frac{60}{10} = 6$$

$$\alpha = 1$$

$$\beta = \frac{1}{Q} = \frac{1}{6} = .1667$$

$$\gamma = 1$$

$$R_1 = \frac{1}{\alpha\beta\omega_o C} = 79.6 K\Omega$$

$$R_2 = \alpha R_1 = 79.6 K\Omega$$

$$R_3 = \frac{1}{\sqrt{\gamma}\omega_o C} = 13.3 K\Omega$$

$$R_4 = \frac{1}{\alpha\omega_o C} = 13.3 K\Omega$$

$$R_5 = \frac{\sqrt{\gamma}}{\alpha\omega_o C} = 13.3 K\Omega$$

$$R_6 = \frac{1}{\omega_o C} = 13.3 K\Omega$$

Appendix C: Typical Test Results

Test 1
Asphalt
Range 180 - 160 mm
Location of Laser 495 mm

Distance	Mean Distance	Std Dev.	Max Dist.	Min Dist.	Range
2592.4	2592.3	0.8	2593.0	2590.9	2.1
2592.8					
2592.8					
2593.0					
2590.9					
2538.4	2537.5	0.9	2538.4	2536.3	2.1
2536.9					
2538.1					
2538.0					
2536.3					
2490.3	2488.5	4.9	2493.3	2482.3	10.9
2493.3					
2492.3					
2484.3					
2482.3					
2237.6	2238.8	1.2	2240.8	2237.6	3.2
2238.2					
2239.1					
2240.8					
2238.5					
2219.4	2220.4	1.1	2221.5	2219.1	2.4
2219.1					
2221.2					
2221.5					
2220.7					
2198.6	2198.7	0.9	2200.1	2198.0	2.2
2198.0					
2198.1					
2200.1					
2198.6					
2107.5	2103.7	2.8	2107.5	2101.2	6.2
2105.9					

2101.6					
2102.4					
2101.2					
2043.2	2044.1	0.7	2044.9	2043.2	1.7
2044.3					
2044.9					
2044.4					
2043.5					
1990.7	1992.7	1.3	1993.8	1990.7	3.1
1992.3					
1993.5					
1993.4					
1993.8					
1948.7	1943.9	2.8	1948.7	1941.6	7.2
1941.6					
1942.6					
1942.8					
1943.7					
1891.5	1891.1	1.4	1892.8	1889.1	3.7
1889.1					
1891.6					
1890.4					
1892.8					
1859.8	1861.6	1.3	1863.3	1859.8	3.6
1862.0					
1861.1					
1861.6					
1863.3					
1816.5	1814.4	3.1	1816.9	1809.3	7.6
1816.9					
1815.4					
1814.2					
1809.3					
1772.3	1772.6	0.5	1773.0	1771.8	1.3
1771.8					
1773.0					
1773.0					
1772.8					

1729.8	1728.3	4.0	1732.3	1723.7	8.5
1731.2					
1732.3					
1723.7					
1724.3					
1689.8	1688.8	3.0	1690.9	1683.5	7.4
1690.4					
1690.9					
1689.4					
1683.5					
1649.0	1650.1	0.9	1651.3	1649.0	2.3
1649.7					
1649.7					
1650.7					
1651.3					
1618.5	1616.6	3.1	1619.4	1611.5	7.9
1616.0					
1619.4					
1617.8					
1611.5					
1581.0	1581.0	1.1	1582.2	1579.1	3.1
1582.2					
1579.1					
1581.1					
1581.5					
1541.7	1542.0	1.1	1543.2	1540.4	2.8
1543.2					
1542.7					
1542.0					
1540.4					

Test 2
 White Paper
 Range 180 - 160 mm
 Location of Laser 495 mm

Distance	Mean Distance	Std Dev.	Max Dist.	Min Dist	Range
2678.2	2678.2	0.1	2678.3	2678.1	0.2
2678.2					
2678.1					
2678.1					
2678.3					
2639.9	2639.9	0.1	2640.0	2639.8	0.2
2640.0					
2639.9					
2640.0					
2639.8					
2590.6	2590.5	0.1	2590.6	2590.5	0.1
2590.6					
2590.5					
2590.5					
2590.6					
2540.7	2540.6	0.1	2540.7	2540.5	0.2
2540.5					
2540.6					
2540.5					
2540.6					
2494.1	2494.1	0.1	2494.2	2494.1	0.1
2494.1					
2494.1					
2494.2					
2494.2					
2452.0	2452.2	0.1	2452.3	2452.0	0.3
2452.2					
2452.3					
2452.2					
2452.1					
2419.2	2419.1	0.1	2419.2	2419.0	0.1
2419.1					

2419.2					
2419.1					
2419.0					
2371.0	2370.9	0.0	2371.0	2370.9	0.1
2370.9					
2370.9					
2370.9					
2371.0					
2326.5	2326.4	0.1	2326.5	2326.3	0.2
2326.4					
2326.4					
2326.3					
2326.4					
2279.5	2279.5	0.2	2279.9	2279.4	0.5
2279.4					
2279.4					
2279.4					
2279.9					
2241.0	2240.9	0.0	2241.0	2240.9	0.1
2240.9					
2240.9					
2241.0					
2240.9					
2198.5	2198.6	0.1	2198.7	2198.5	0.2
2198.7					
2198.6					
2198.7					
2198.7					
2154.1	2154.1	0.0	2154.2	2154.1	0.1
2154.2					
2154.1					
2154.1					
2154.1					
2106.8	2106.7	0.1	2106.8	2106.6	0.2
2106.7					
2106.8					
2106.6					
2106.7					

2069.3	2069.3	0.1	2069.5	2069.1	0.3
2069.5					
2069.3					
2069.1					
2069.2					
2020.9	2021.0	0.1	2021.2	2020.9	0.3
2021.2					
2021.0					
2021.0					
2021.0					
1987.5	1987.4	0.1	1987.5	1987.3	0.2
1987.4					
1987.4					
1987.4					
1987.3					
1930.2	1930.0	0.1	1930.2	1930.0	0.2
1930.0					
1930.0					
1930.0					
1930.0					
1900.0	1900.0	0.1	1900.1	1899.8	0.2
1900.1					
1900.0					
1900.0					
1899.8					
1850.8	1850.9	0.1	1851.0	1850.8	0.2
1850.8					
1851.0					
1850.9					
1850.9					

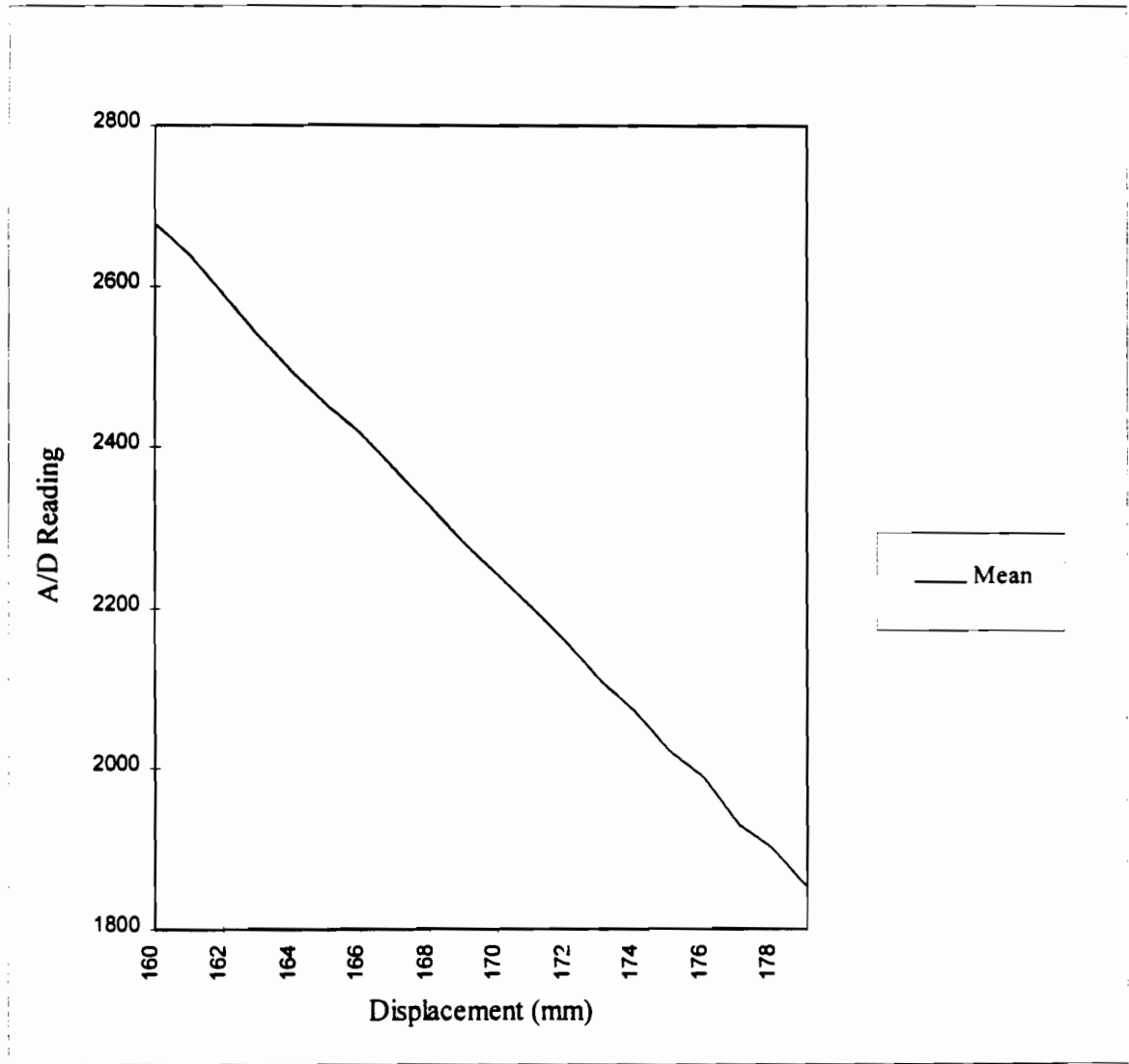


Figure 18. Plot of Test 2 Mean Displacement Readings Versus Displacement Distance